Indian Journal of Pure & Applied Physics
Vol. 57, July 2019, pp. 475-482

Influence of Cu concentration on the structural, morphological, optical and catalytic properties of TiO_2 thin films

R Vidhya[a], R Gandhimathi[b], M Sankareswari[a] & K Neyvasagam[c*]

[a]Department of Physics, V V V College for women, Virudhunager 626 001, India
[b]Department of Physics, AMET University, Kanathur, Chennai 603 112, India
[c]Department of Physics, The Madura College, Madurai 625 011, India

Received 28 May 2017; accepted 29 April 2019

Pristine titanium oxide (TiO_2) and Cu doped TiO_2 thin films of ~2.0 µm thicknesses have been deposited on glass substrates by sol-gel dip coating technique. The deposited films are even and more adherent to the substrate. The consequences of incorporation of Cu ions of different concentration in TiO_2 lattice towards the structural, morphological and optical characteristics of prepared thin films have been investigated. Cu doping alters crystallite size and morphology of doped TiO_2 films marginally. Gradual increase in concentration of Cu atoms into TiO_2 matrix expands the absorption window of prepared films to visible region. The decrease in excitonic energy upon Cu doping promotes the charge separation in TiO_2 semiconductor. Depending upon Cu concentration, exciton life time is extended fairly which leads to improved electron-hole separation and enhanced oxidation-reduction reactions at the surface of TiO_2 semiconductors. The advantage of thin film catalyst over the other catalyst structures has been exhibited by the reusability nature of Cu-TiO_2 films. This study reveals that an ideal amount of Cu doping can increase the photocatalytic performance of TiO_2 thin films efficiently.

Keywords: Cu-TiO_2 thin films, Photocatalysis, Sol-gel method, XRD, AFM

1 Introduction

Titanium dioxide (TiO_2) is a renowned chemically stable and harmless material which is used extensively in various fields[1-3] such as surface coating, photoelectrodes, paints, cosmetics and so on. In recent years, it has received a great deal of attention as a most excellent photocatalytic material[4, 5]. The photo-induced decomposition and photo-induced hydrophilicity properties of TiO_2 make it useful in environmental purification[6]. Moreover, the other utilizations such as antibacterial, antipollution and deodorization are also possible because of these unique photocatalytic mechanisms of titania. Pristine TiO_2 (band gap ~3.2eV) rely on ultraviolet-light irradiation to fulfill its photocatalytic functions so the TiO_2 photocatalyst faces its own limitations in effective use of light. In order to enhance the photocatalytic efficiency of TiO_2 and project this material as a visible-light-responding photocatalyst, noble metal oxides or transition metals or non-metallic elements can be added as a dopant into the matrix of TiO_2[7, 8]. Specifically, incorporation of metal impurities in the metal oxide structures extends its absorption edge to visible region and creates self-excited trapping centers and oxygen vacancies which improve the excitation of electron hole pair. The photo excited electrons generated by the metal dopant are transferred to the conduction band of metal oxide semiconductor, resulting an enhanced photocatalytic process[9-16].

Doping of TiO_2 with metals like Au, and Ag not only increases the surface area of the active region but also promotes the optical and chemical properties of the same[17-20]. Other than noble metals, Cu is the best appropriate metal dopant to extend its absorption edge to longer wavelength. The incorporation of copper ions into the TiO_2 matrix accelerates the photoreaction of the catalyst as the Cu dopant intensifies oxygen adsorption on the surface of the sample[21,22]. As a result, the heterogeneous photocatalyst Cu doped TiO_2 can remove persistent organic pollutants as well as microorganisms present in the water effectively. The chemical composition ratio of dopant and TiO_2 is an important factor in determining degradation efficiency of samples. To extract complete photocatalytic ability of TiO_2, metal dopant concentration can be

*Corresponding author (E-mail: srineyvas@yahoo.co.in)

varied inside TiO_2 environment. Also, the efficiency of catalyst relies on the ability of adsorption of contaminated molecule on the surface of catalyst since thin films with appropriate thickness, deposition uniformity; larger active surface area and high crystallinity are preferred for photocatalytic applications. Thin film photocatalyst consists of huge number of adsorption sites per unit surface area rather than the powder photo catalyst. Apart from that thin film photocatalysts are convenient to use and recyclable[23]. In the present study, efforts have been made to deposit undoped and Cu-doped TiO_2 thin films via sol gel technique. We explored the variation in structural, morphological and optical properties of samples upon increase in Cu doping. Also, the concentration and effect of Cu additives on photodegradation of methylene blue executed by oxidation-reduction method was reported successfully.

2 Experimental

2.1 Preparation method

The physical properties of thin films are highly dependent on various parameters such as deposition time, thickness, chemical composition, geometry and annealing temperature. Thin films with good homogeneity, controlled composition, low processing temperature, large area coatings are required for photocatalytic applications. In this work, sol gel dip coating method was used to prepare thin films on glass substrates. For the preparation of the sol solution; Firstly, the mixture of precursor titanium tetra isopropoxide (TTIP), ethanol (C_2H_5OH), and acetic acid was stirred for 30 minutes. The dopant precursor copper II nitrate trihydrate of 0.02 mol% dissolved in ethanol was added with the above mixture and the whole solution was stirred for another one hour. The 0.02% mol Cu doped TiO_2 sol was deposited on glass substrates by dip coating process at room temperature with the drawing speed of about 1.5 mm/s and the process was repeated 7 times to obtain thickness of 2 μm. The coated samples were dried at 100 ºC for 10 min. The same procedure was repeated for preparing 0.03, 0.04 and 0.05 mol% of Cu doped TiO_2 thin films. Also, pure TiO_2 thin film was prepared using the same procedure without adding any copper precursor. The prepared films were annealed at 400 ºC for 3 h to obtain better crystallinity. The semitransparent films with 7-layer coating were employed for further characterization.

2.2 Characterization

The crystallite size of the Cu-TiO_2 thin films prepared with different Cu concentrations was estimated by X–ray diffraction method (XRD) using X'PERT PRO X–ray diffractometer which was operated at 40 KV and 30 mA with $CuK\alpha_1$ radiation of wavelength 1.5407 Å. UV–visible spectra were recorded in the range of 300 – 800 nm using the Schimadzu 1800 UV–VIS – NIR spectrophotometer. The surface morphology observation and elemental analysis were done by Carl Zeiss and Supra 55, respectively. Surface roughness of the films was recorded using NT-MDT, NTEGRA Prima-Modular AFM in semi contact mode using SiN cantilever. Photocatalytic activity of the prepared TiO_2 and Cu-TiO_2 thin films was studied by examining the degradation of aqueous solution of methylene blue (MB) under visible light irradiation using 500-W halogen lamp.

3 Results and Discussion

3.1 Structural analysis

The prepared polycrystalline thin films have subjected to X- ray diffraction analysis. The XRD pattern of undoped TiO_2 and Cu doped TiO_2 thin films are shown in Fig. 1 (inset). The diffraction patterns depict that all thermally treated (at 400 °C) Cu-TiO_2 films have tetragonal crystal structure with the anatase phase. The lattice parameter values 'a' and 'c' are in good agreement with the standard TiO_2 single crystals (a = 3.785 Å, c = 9.513 Å) (JCPDS card no 89-4203)[24]. The characteristic peaks of the pristine TiO_2 and Cu-TiO_2 films are found at 2θ values of 25.38°, 37.87°, 48.01° and 53.95° corresponding to

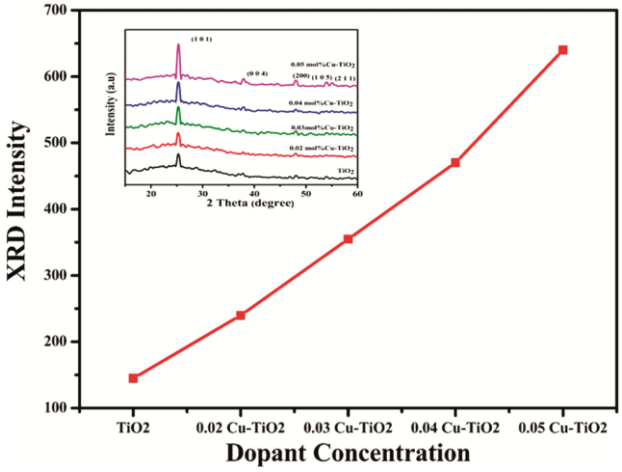

Fig. 1 — Dopant concentration vs XRD intensity.

the (*hkl*) planes (101), (210), (200) and (105), respectively. No distinct peaks were found for copper. However, a subtle shift in (101) reflection plane of Cu doped TiO_2 films to higher diffraction angle relative to pure TiO_2 was identified which confirms the incorporation of dopants. The addition of Cu doesn't bring any structural transition (phase change) in prepared films. Nevertheless, it could be noted that the intensity of XRD pattern increases with the rise of Cu concentration as shown in Fig. 1. Increase in the intensity may be attributed to the change in crystallite size of Cu doped TiO_2 single crystals. The gradual increase of Cu concentration into TiO_2 matrix suppresses crystallite size accordingly. The average crystallite size was computed using Scherrer's formula[25]:

$$D = \frac{k\lambda}{\beta cos\theta} \quad \ldots (1)$$

Where D is the crystallite size, k is a constant, λ is the wavelength of X-ray diffraction, β is FWHM, θ is the angle of diffraction. The grain size of TiO_2 was estimated to be in the range of 53-64 nm. Decreased crystallite size is the good indication of increased surface area. The lattice strain (ε) provoked by the dopant is calculated, using the relation:

$$\varepsilon = \frac{\beta cos\theta}{4} \quad \ldots (2)$$

The value of dislocation density (δ) is calculated, using the relation:

$$\delta = \frac{1}{D^2} \quad \ldots (3)$$

It was also seen that the stress produced by the variation in the ionic radius of Ti and Cu increases strain and dislocation density in Cu-TiO_2 particles with the raise of dopant concentration[26]. The measured structural parameters are list in Table 1. Thus, depending upon the amount of Cu atoms, structural deformation has been stimulated in the prepared Cu-TiO_2 films. Anatase phase and increased surface area of Cu doped TiO_2 films can engage more charge carriers to participate in surface reactions[27].

3.2 Morphological analysis

3.2.1 Surface morphology

To understand microscopic properties of metal oxide surface, it is necessary to identifying the surface defects of the prepared films. The FESEM picture of pristine TiO_2 thin film annealed at 400 °C is shown in Fig. 2 (a). It was seen that the undoped TiO_2 consists evenly distributed TiO_2 spherical particles of size (~36-140 nm) on the surface of the film. The spherical particles are due to the aggregation of tiny TiO_2 crystals[28]. FESEM image of prepared Cu-doped TiO_2 is shown in Fig. 2 (b). It was noticed that Cu-doped

Table 1 — Structural parameters of TiO_2 and Cu doped TiO_2 thin films.

Sample	D × 10^{-9} m	δ × 10^{14} lines/m^2	ε	Lattice parameters Å	
				a	c
Undoped TiO_2	64.52	2.402	0.0309	3.777	9.501
0.02 mol % Cu	60.78	2.71	0.0328	3.7928	9.4787
0.03 mol % Cu	58.26	2.947	0.0342	3.7894	9.5035
0.04 mol % Cu	55.72	3.2209	0.0358	3.7884	9.545
0.05 mol % Cu	53.29	3.5219	0.0374	3.785	9.8647

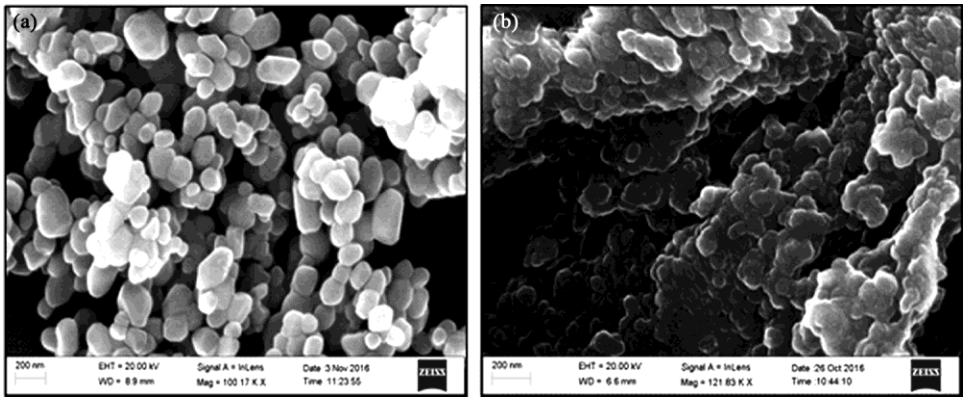

Fig. 2 — FE-SEM micrographs of prepared samples: (a) TiO_2 thin film, (b) 0.05mole% Cu-TiO_2 thin film.

TiO_2 has a slightly smaller particle size (~32-70 nm) than that of pure TiO_2. In addition, agglomeration of Cu-TiO_2 particles is quite larger because adding Cu dopant alters the surface morphologies and roughness of the TiO_2 films. Also, increase in Cu concentration affects the grain growth (grain size reduction)[29]. This kind of change in morphology and grain size leads to modification in optical properties of the thin films.

EDX technique was used to find out the composition of pristine TiO_2 and Cu-TiO_2 thin films. Fig. 3 (a and b) shows the EDX images of the pristine TiO_2 and Cu-TiO_2 thin films. It was seen that the pure TiO_2 film shows the composition of Ti and O elements. As well Cu-TiO_2 thin films depict stoichiometric composition of Ti, O and Cu elements. Other elements observed might be due to their presence in the glass substrate

3.2.2 Surface topography

Atomic force microscopy images of pure and 0.05 mol% Cu doped TiO_2 thin films are shown in Fig. 4 (a – b). The area covered on the film for imaging is

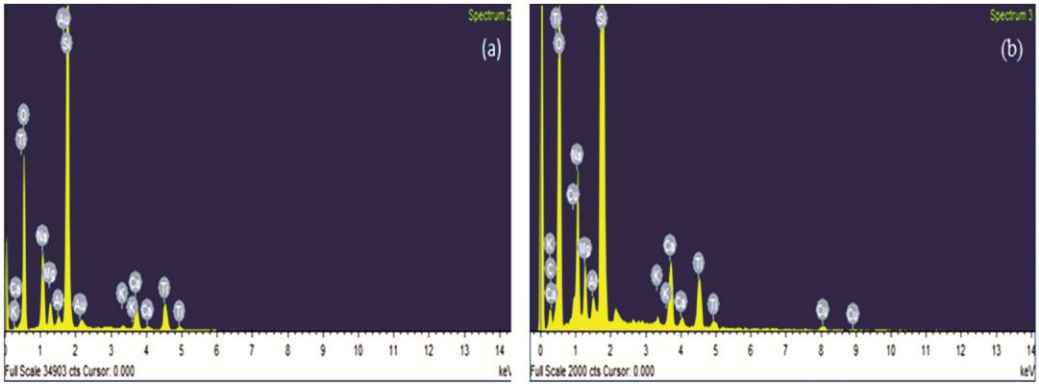

Fig. 3 — EDX spectrum of pure TiO_2 and 0.05 mole% Cu doped TiO_2 thin films.

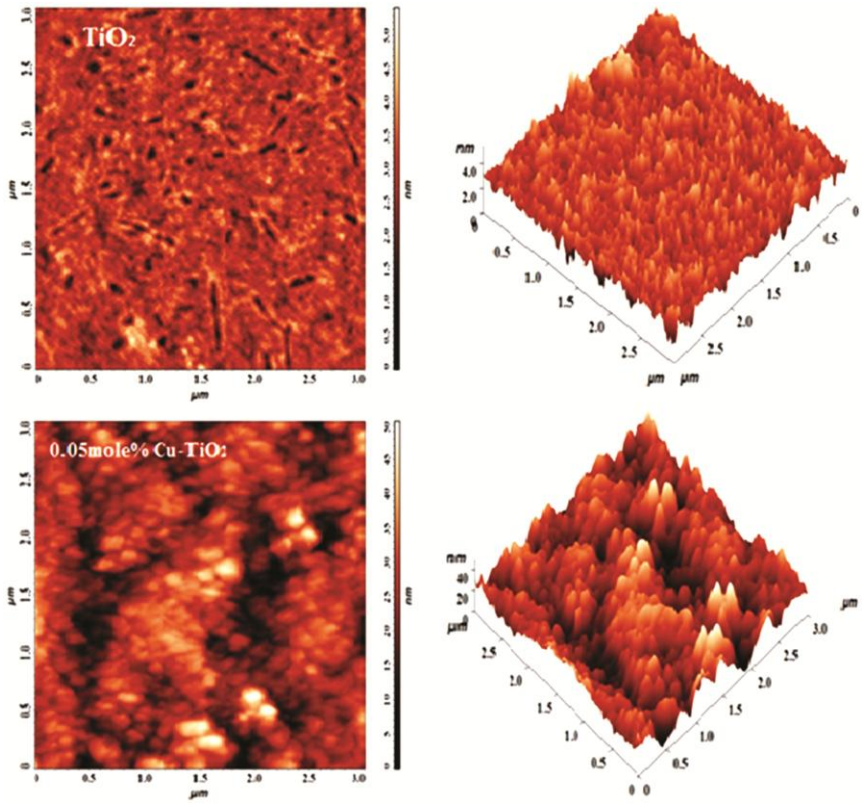

Fig. 4 — AFM image of (a) TiO_2 and (b) 0.05 mole% Cu doped TiO_2 thin films.

3 µm × 3 µm. The surface plots of pure TiO_2 reveal the distribution of grains with randomly oriented pores. The columnar arrangement of TiO_2 grains found in 3D image indicates the growth along the c-axis perpendicular to the substrate surface. Figure 4 (b) depicts the distribution of spherical shaped grains on the surface of the films. The white color represents existence of Cu atoms in TiO_2 lattice. Also, a small cluster formation was detected from the surface plot since increase in Cu concentration leads to agglomeration of grains. The development of island structures in Cu doped film is shown in Fig. 4 (b), 3D image. In doped films too, grain growth is along the c-axis[30]. As well it visualizes that the inclusion of Cu additive in the TiO_2 showed a significant change in roughness. The observed surface roughness value of pure and doped thin films are about 0.38818 nm and 5.7137 nm, respectively, which predicts evidently the increase of roughness value with Cu doping.

3.3 Optical performance of TiO_2 and Cu-TiO_2 thin films

Figure 5 (a) shows UV-Vis transmittance spectra of pure TiO_2 and Cu doped TiO_2 thin films. The transmittance of all films was found to be small in the UV region and more in the visible region. It is also viewed that transmittance of the films decreases with increasing concentration of the Cu metal dopant (0.02 to 0.05 mol %). Because at higher doping concentration, a greater number of atoms (orbital electrons) are present on the film surface. As a result, energy levels available for the photons to be absorbed are large as well. In other words, the scattering of photons on the film surface increases due to increased crystal defects produced by the dopant which leads to decrease in transmittance of the Cu doped TiO_2 thin films[31]. It is clearly seen that the cut off wavelength of doped TiO_2 films shows red shift from the cut off wavelength of pure TiO_2. Thus, the optical properties of TiO_2 were tuned towards the visible light by the substitution of Ti^{4+} by Cu^{2+} ions.

The optical band gap of the absorption peak was obtained by extrapolating the linear portion of $(\alpha h\upsilon)^{1/2}$ versus hυ curve (i.e. Tauc plot equation)

$$(\alpha h\vartheta) = A(h\vartheta - E_g)^n \quad \ldots (4)$$

Where E_g is the optical band gap of the films and A is a constant. It is found that all samples had indirect band gap. Yet the wide band of pure TiO_2 2.96 eV decreases to 2.62 eV with the increase in Cu content (~400 meV shift) since the existing interaction potential between free electrons of Cu dopant and TiO_2 varies with the dopant concentration. The change in interaction potential leads to reduction in energy gap. Also, the discrepancy in film density and grain size might be another cause for the decline in band gap of Cu doped TiO_2 films.

3.4 Photoluminescence study

To explore the luminescent properties of prepared samples, films were subjected to photoluminescence measurements at room temperature. The wavelength of excitation beam used is 410 nm. The room temperature emission spectra of undoped and Cu doped thin films are shown in Fig. 6. The spectra demonstrate strong visible emission peaks at 488 nm and 560 nm, respectively. The blue emission peak at 488 nm is attributed to the deep level emission of transition metal oxides[32]. The formation of oxygen vacancies or F centres in the vicinity of metal oxide surface is due to the point defects created by various

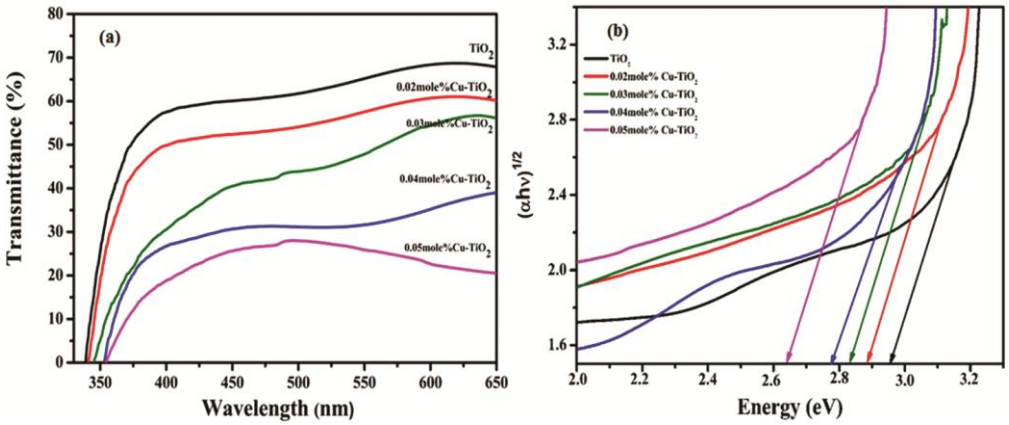

Fig. 5 — (a) Optical transmittance spectra of TiO_2 and Cu doped TiO_2 thin films; (b) variation of $(\alpha h\vartheta)^{1/2}$ versus (hν) of pure TiO_2 and Cu doped TiO_2 thin films.

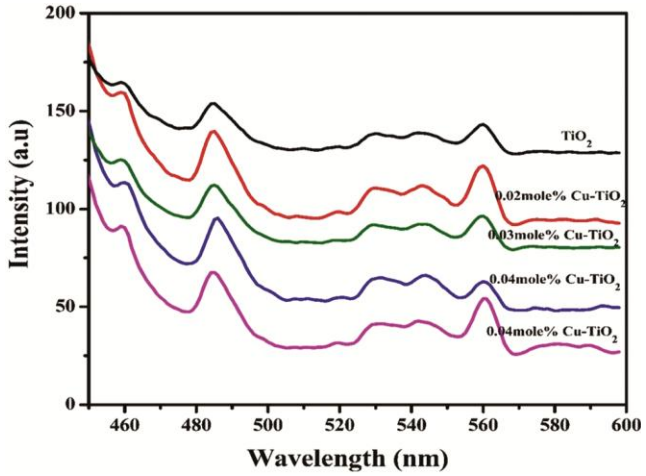

Fig. 6 — Photoluminescence spectra of pure TiO_2 and Cu doped TiO_2 thin films.

effects and these oxygen vacancies act as radiative centers during the luminescence processes[33]. Here doping of Cu atoms, leads to formation of more oxygen vacancy cites on the surface of the films since the energy required to form oxygen vacancy by Cu ions is much lower. The oxygen vacancy has important role on catalytic activity of the Cu-TiO_2 films too[34, 35]. The appearance of green emission peak at 537 nm is due to the other induced surface defects[36]. It is also seen that undoped TiO_2 show high intensity where the intensity of the doped TiO_2 film peaks decreases on doping with Cu. The intensity of highest excitation peak of 0.05% mol Cu doped TiO_2 thin film was 2.3 times smaller than the intensity of highest excitation peak of pure TiO_2 film. The decline in PL emission intensity is possibly because of delayed of recombination of the photo generated electron–hole pairs and more charge separation in highly doped samples. Effective utilization of these photoinduced excitons leads to significant progress in photocatalytic degradation process of Cu-TiO_2 films.

3.5 Degradation of methylene blue (MB)

During irradiation excitons with the sufficient life time diffuse the surface of the film and involve in reduction reaction. The photo degradation activity of pure TiO_2 and Cu doped TiO_2 thin films was analyzed by decomposing methylene blue dye (MB) solution under visible light irradiation. In order to carry out the process, 3 µml of methylene blue dye was dissolved in 30 ml water and taken in a 50 ml beaker. The schematic diagram of photocatalytic degradation of Cu-TiO_2 is shown in Fig. 7. The films to be analyzed were immersed into the solution and kept under 500W

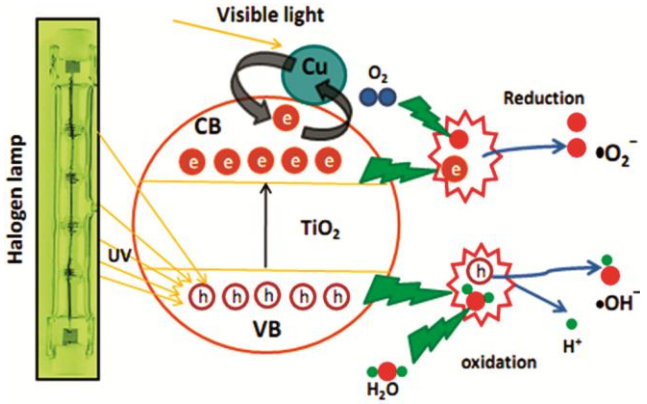

Fig. 7 — Photo catalytic degradation schematic diagram.

halogen lamp for 0, 1, 2, 3 and 4 h, respectively. The absorbance of the photo degraded solution was recorded using Schimadzu-1800 UV-Vis spectrometer. The results of photocatalytic activity of undoped, 0.03 % and 0.05 % Cu doped TiO_2 films are plotted and shown in Fig. 8 (a – c), respectively. The characteristic absorption peak of methylene blue was found at 668 nm in all spectra. The absorption spectra of MB show high absorbance for pure TiO_2 thin film which indicates low photo bleaching effect of TiO_2 thin films. However, the absorption spectra of MB depict low absorbance value at 668 nm for other Cu doped TiO_2 films. The TiO_2 films doped with Cu content of 0.02 %–0.05 % show improved photocatalytic performance. In particular, 0.05 % Cu doped TiO_2 exhibits the best photocatalytic performance among all. The absorbance spectrum of MB for 0.05 % Cu doped TiO_2 shows almost a straight line at 4 h, i.e., enhanced light harvest (or very low absorbance) together in UV and visible light regions. The reason is that the impurity energy level created by the metal dopant Cu separates photo induced excitons effectively. And the electron can be transferred from the conduction band of TiO_2 to metallic copper ion easily because of the overlapped band gap of metal dopant. Also, the induced oxygen vacancies act as the active sites on the surface of TiO_2 for water dissociation. It delays the recombination of hole electron pairs. Thus, the combined exploitation of UV-V is light and improved charge separation of 0.05% Cu-doped TiO_2 thin films make it as a best photocatalyst compared to other films[37-39]. It was also found that 0.05% Cu is an optimum dopant level in TiO_2 matrix which shows effective separation of photo induced electron hole pair. The degradation efficiency of the MB was calculated by:

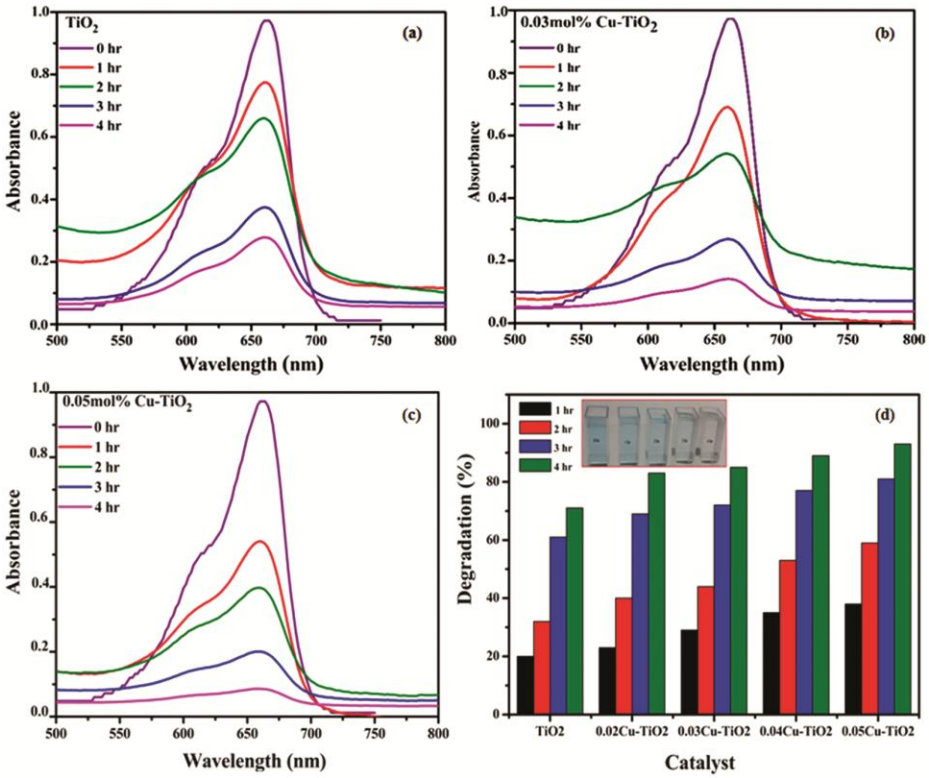

Fig. 8 — Photo degradation of methylene blue using TiO_2 and Cu-TiO_2 thin films.

$$\% \text{ D} = \frac{A_0 - A_t}{A_0} \times 100 \quad \ldots(5)$$

Where A_0 is the initial absorbance and A_t is the absorbance after time t. The degradation efficiency of prepared samples is displayed in Fig. 8d. It could be noticed that 0.05 % Cu-TiO_2 demonstrates about 80 % degradation at 4 hr.

3.6 Reusability of the film

One of the important features of thin film catalyst is its reusability. This catalyst could be easily recovered by cleaning with water and reused without loss of its catalytic activity[40, 41]. Hence to calculate Cu-TiO_2 catalyst stability, the film was undergone with 6 cycles of photo degradation in MB dye under visible light irradiation. Here, we report the reusability of 0.05 mol% of Cu-TiO_2 thin film. After each cycle, the film was washed with distilled water, dried in air and reused in same conditions. The catalytic efficiency was evaluated in each cycle. It was noticed that it maintains its excellent catalytic efficiency even after 6 cycles with a small loss which is shown in Fig. 9. The Cu-TiO_2 thin film (0.05 mol %) was preferred for testing the reusability since it showed the improved catalytic performance than all other prepared films in degradation of dyes.

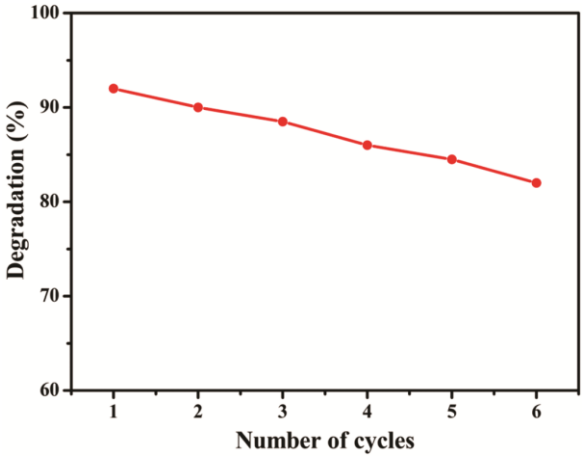

Fig. 9 — Reusability of 0.05mole% Cu-TiO_2 thin film.

4 Conclusions

Undoped and Cu doped TiO_2 thin films were deposited on glass substrates by sol-gel dip coating technique. The results imply that varying Cu content facilitates the possibility of modifying the structural, morphological and optical properties in TiO_2 thin films remarkably. The crystallite sizes of the deposited samples are decreasing upon Cu doping. The absorption spectrum of doped TiO_2 films shows a progressive red shift with respect to the undoped

films. The results also revealed that the measured optical band gap values of the prepared films decrease on increasing Cu concentration. The Cu mediated withdrawal of hydroxyl radicals in prepared films exhibit enhanced photocatalytic activity. Therefore, with the systematic incorporation of Cu atoms in TiO_2 lattice, the prepared thin films show improved crystallinity, increased surface area, large visible light response and proficient catalytic activity. Furthermore, the results support in exploring potential applications of reusable Cu/TiO_2 thin films as a promising photocatalyst for commercialization.

References

1 Chen X, *Chem Rev*, 114 (2014) 9281.
2 Liu L & Chen X, *Chem Rev*, 114 (2014) 9890.
3 Chneider J, Matsuoka M, Takeuchi M, Zhang J, Horiuchi Y, Anpo M & Bahnemann D, *Chem Rev*, 114 (2014) 9919.
4 Rajh T, Dimitrijevic N M, Bissonnette M, Koritarov T & Konda V, *Chem Rev*, 114 (2014) 10177.
5 Bai Y, Mora-Seró I, De Angelis F, Bisquert J & Wang P, *Chem Rev*, 114 (2014) 10095.
6 Snehamol M, Priyanka G, Stephen R, Vignesh K, Ciara B, Hinder S J, John B, Michael N & Pillai S C, *Appl Sci*, 8 (2018) 2067.
7 Javier N, Antonio Sa´nchez C, Teresa A, Norge C, Herna´ndez, Desiree´ M de los Santos, Jesu´s Sa´nchez-Ma´rquez, David Zorrilla, Concha Ferna´ndez-Lorenzo, Rodrigo Alca´ntara & Joaquı´n Martı´n-Calleja, *Phys Chem Chem Phys*, 16 (2014) 3835.
8 Linhui Y, Yangming L, Jing H, Sen L & Danzhen L, *J Am Ceram Soc*, 1-8 (2016) 1.
9 Wei S, Rui Z & Shukai Z, *Matéria (Rio J)*, 21 (2016) 301.
10 Vibhu B & Amit D, *J Environ Chem Eng*, 4 (2016) 1267.
11 Reda S M, Khairy M & Mousa M A, *Arab J Chem*, (2017).
12 Asahi R, Morikawa T,Ohwaki T, Aoki K & Taga Y, *Science*, 293 (2001) 269.
13 Maeda M & Watanabe T, *J Electrochem Soc*, 153 (2006) 186.
14 Maeda M & Hirota K, *Appl Catal A: Gen*, 302 (2006) 305.
15 Xiang L, Zhao X, Shang C &Yin J, *J Colloid Interface Sci*, 403 (2013) 22.
16 Awazu K, Fujimaki M, Rockstuhl C, Tominaga J, Murakami H, Ohki Y, Yoshida N & Watanabe T, *J Am Chem Soc*, 130 (2008) 1676.
17 Nigussie G Y, Tesfamariam G M, Tegegne B M, Weldemichel Y A, Gebreab T W, Gebrehiwot D G & Gebremiche G E, *Int J Photoenergy*, 2018 (2018) 5927485.
18 Manoranjan S, Bing W, Liying Z, Craig J, Wei-Ning W, Kristen J, Yogesh G, Yinjie J & Pratim B, *Nanotechnology*, 22 (2011) 415704.
19 Chiu W, Khiew P, Cloke M, Isa D, Tan T, Radiman S, Abd-Shukor R, Hamid M, Huang M & Chia C, *Chem Eng J*, 158 (2010) 345.
20 Milenova K I, Eliyas A E, Blaskov V N, Avramova I A, Stambolova I D, Karakirova Y D, Vassilev S V, Nikolov P M, Kasabova N A & Rakovsky S K, *Bulg Chem Commun*, 47 (2015) 336.
21 Patil A & Pathan I J, *J Nano-Electron Phys*, 3 (2011) 433.
22 Colón G, Maicu M, Hidalgo M C & Naïve J A, *Appl Catal B: Environ*, 6 (2006) 41.
23 Singh A K & Nakate U T, *ISRN Nanotechnol*, 2014 (2014) 1.
24 Zuas O & Budiman H, *Nano-Micro Lett*, 5 (2013) 26.
25 Dhage S R, Gaikwad S P & Ravi V, *Mater Sci*, 27 (2013) 487.
26 Manoharan C, Pavithra G, Bououdina M, Dhanapandian S & Dhamodharan P, *Appl Nano Sci*, 6 (2015) 815.
27 Luttrell T, Halpegamage S, Tao J, Kramer A, Sutter E & Batzill M, *Sci Rep*, 4 (2014) 4043.
28 Das K, Ray S, Chaudhuri S & Maity A B, *Indian J Pure Appl Phys*, 47 (2009) 377.
29 Weng W, Ma M, Du P, Zhao G,Shen G, Wang J & Han G, *Surf Coat Technol*, 198 (2005) 340.
30 Karunakaran C, Abiramasundari G, Gomathisankar P, Manikandan G & Anandi V, *J Colloid Interface Sci*, 352 (2010) 68.
31 Rajendran V & Anandan K, *Mater Sci Semicon Proc*, 15 (2012) 393.
32 Pacchioni G, *Chem Phys Chem*, 4 (2003) 1041.
33 Wahlström E, Lopez N, Schaub N, Thostrup P, Rønnau A, Africh C, Lægsgaard E, Nørskov J K & Besenbacher F, *Phys Rev Lett*, 90 (2003) 026101.
34 Carrasco J, Lopez N, Illasa F & Freund H J, *J Chem Phys*, 125 (2006) 074711.
35 Jiajun W, Qiangqiang M, Jing H, Qunxiang L & Jinlong Y, *J Chem Phys*, 140 (2014) 174705.
36 Schaub R, Thostrup P, Lopez N, Lægsgaard E, Stensgaard I, Nørskov J K & Besenbacher F, *Phys Rev Lett*, 87 (2001) 266104.
37 Jenny S, Masaya M, Masato T, Jinlong Z, Yu H, Masakazu A & Bahnemann D W, *Chem Rev*, 114 (2014) 9919.
38 Mahnaz A & Nasrollah N I, *Silicon*, 10 (2018) 2569.
39 Razali M H, Ahmad-Fauzi M N, Mohamed A R & Sreekantan S, *Adv Mater Res*, 911 (2014) 126.
40 Mahtab P, Adel M G, Zarrin G & Sajjad A K, *Arab J Chem*, 1 (2016).
41 Pang Y L & Abdullah A Z, *J Hazard Mater*, 235 (2012) 326.